

## Electronic structure of Si(111)-B( $\sqrt{3}\times\sqrt{3}$ )R 30° studied by Si 2*p* and B 1*s* core-level photoelectron spectroscopy

A. B. McLean, L. J. Terminello, and F. J. Himpsel

*IBM Research Division, Thomas J. Watson Research Center, P.O. Box 218, Yorktown Heights, New York 10598*

(Received 13 October 1989)

An investigation of the Si(111)-B( $\sqrt{3}\times\sqrt{3}$ )R 30° system has been performed using high-resolution photoelectron spectroscopy of the Si 2*p* core level and polarization-dependent studies of the B 1*s* absorption edge. Least-squares analysis of the Si 2*p* core-level line shape reveals that it comprises a bulk component and a surface component shifted by  $0.40\pm 0.02$  eV to higher binding energy. The exceptionally large surface-to-bulk ratio that is observed in this system suggests that the range of influence of the B atoms extends to more than 1 monolayer of Si atoms. The magnitude of the surface-to-bulk ratio is consistent with a model in which B occupies a subsurface site below a Si adatom. The B 1*s* edge contains a feature which is excited by the component of the electric field vector perpendicular to the surface. We argue that this arises from an electronic transition from the B 1*s* level into an empty surface orbital, orientated perpendicularly to the surface. We also study the change of the electronic structure as the surface is covered with Si, thereby producing a buried  $\delta$ -doping layer.

### I. INTRODUCTION

Although the column-III metals (e.g., Al, Ga, In) are known<sup>1</sup> to stabilize a ( $\sqrt{3}\times\sqrt{3}$ )R 30° reconstruction on the Si(111) surface, it has recently been discovered that B stabilizes a  $\sqrt{3}\times\sqrt{3}$  structure which may have a different structural origin.<sup>2-10</sup> All of the adsorbates mentioned above are thought to occupy the  $T_4$  adatom site, above a second-layer silicon atom, and saturate three broken bonds on the first Si(111) layer. In contrast, it appears as if B (Refs. 2-10) may occupy the substitutional site in the uppermost Si bilayer beneath the  $T_4$  adsorption site which is in turn occupied by a Si atom. It has been shown, for example, that the ( $\sqrt{3}\times\sqrt{3}$ )R 30° low-energy electron diffraction (LEED) pattern is preserved after a room-temperature 1-Å deposit of Si (e.g., Ref. 6), suggesting that the B atoms are incorporated. This is not the case for metals which occupy the adatom site, such as Ga.<sup>6</sup>

The electronic structure of this system also appears to be different from the other  $\sqrt{3}\times\sqrt{3}$  systems. For example, a pseudopotential total-energy minimization calculation of this surface structure and a momentum-resolved inverse-photoemission study<sup>8</sup> have both identified a strong unoccupied electronic band  $\approx 1.5$  eV above the Fermi level associated with the Si adatoms in the  $T_4$  site. Therefore, the available experimental and theoretical evidence point towards the existence of a new surface structure.

This surface structure is clearly an interesting candidate for core-level photoemission spectroscopy, and we have examined the chemical environment around the Si and B atoms using both Si 2*p* and B 1*s* core-level photoelectron spectroscopy and core-to-valence transitions

from the B 1*s* core level. Analysis of the Si 2*p* core level allows us to extract the magnitude of the surface and bulk components of the Si 2*p* level and also determine the Fermi-level pinning at the surface. The relative intensities of the surface and bulk levels suggests that the range of influence of the incorporated B atoms extends to at least  $\approx 2$  monolayers (ML) of Si atoms. Furthermore, the B absorption edge exhibits a polarization-dependent transition, which we assign to a final state corresponding to the empty adatom orbital. The fact that it is seen at the B edge implies that this orbital has significant weight not only at the Si adatom, but also at the B atom underneath, in agreement with first-principles band-structure calculations.<sup>8,9</sup>

Another interesting aspect of this structure is that it provides the opportunity to create an atomically sharp doping layer ( $\delta$  doping) by growing Si epitaxially on top. We have performed an exploratory first step by growing Si on top of the B( $\sqrt{3}\times\sqrt{3}$ )R 30° structure. In order to prevent interdiffusion and island formation we have employed a chemical-vapor deposition (CVD) method with disilane instead of molecular-beam epitaxy. It is found that the structure at the B absorption edge loses its polarization dependence, as one would expect from the tetrahedral bulk position of a bulk B dopant.

### II. EXPERIMENTAL DETAILS

The angle-integrated core-level photoemission experiments were performed using an ellipsoidal mirror spectrometer<sup>11</sup> coupled to a 6-m-10-m monochromator.<sup>12</sup> During the course of these studies both the 6-m and the 10-m monochromator configurations were used. The former was used to study the Si 2*p* core level and the latter was predominantly used to study the relatively

deep B 1s level and the B 1s absorption edge.

The surfaces were prepared by repeatedly annealing heavily B-doped Si(111) wafers ( $2\times 10^{19}$  cm $^{-3}$ ) to  $\approx 1050^\circ\text{C}$  for 10–20 s in ultrahigh vacuum ( $\approx 2\times 10^{-10}$  Torr). This desorbed the surface oxide and caused B to diffuse from the bulk and segregate at the surface. The amount of surface B could be monitored directly using the B 1s core level and also inferred from the intensity of the B-Si “surface” component in the Si 2*p* core level. Typically five–ten annealing cycles were necessary to saturate the surface structure. Once the surfaces had been prepared they were relatively inert and remained clean, as judged from the absence of photoemission from the O 1s level, for several hours.

### III. Si 2*p* CORE-LEVEL PHOTOEMISSION

The Si(111)-B( $\sqrt{3}\times\sqrt{3}$ )R30° surface structure gives rise to a remarkably simple Si 2*p* core-level photoemission line shape, which suggests that the surface region is highly ordered. In fact, the total Si 2*p* line shape can easily be modeled using only two spin-orbit split doublets (Fig. 1). One of these is the bulk Si component and the other, at higher binding energy, is the component produced by Si-B bonding. The fact that there is only one surface component produced by the Si-B bonding suggests either that there is only one B adsorption site or that the B adsorption sites are energetically undistinguishable. Moreover, the magnitude and polarity of the core-level shift are consistent with a simple model based only on initial-state charge transfer from Si to B.<sup>13</sup> Boron is more electronegative than Si, it draws electrons from Si and thereby lowers the core levels of Si.

In Fig. 1 the effect of annealing the surface is illustrated. The lower curve was collected from a surface that had not reached saturation. The total line shape is modeled using two Gaussian-broadened spin-orbit-split Lorentzian doublets (Voigt functions), separated by  $0.40\pm 0.02$  eV. Subsequent annealing cycles, to  $1050^\circ\text{C}$  for approximately 10–20 s, saturated the surface and produced the upper curve of Fig. 1. The Si-B component grows gradually until it is  $\approx 1.60$  times the area of the bulk component. The magnitude of the Si-B surface component is unusually large, larger than for any other adsorbate on Si,<sup>13</sup> and this suggests that there are a large number of Si–B bonds in the surface region. For comparison, the intensity of the Si 2*p* core-level emission from the outer chain atoms on the Si(111)-(2 $\times$ 1) surface is only approximately one third of the Si 2*p* bulk component under similar conditions.<sup>13</sup>

The photon energy dependence of the total Si 2*p* core-level line shape was studied using the tuneable nature of synchrotron radiation. In Fig. 2 we present the results of measuring the Si 2*p* core level at 110, 120, 130, and 140 eV, together with the results of a least-squares analysis of the core-level line shape. Although the spectra were collected from a surface that was not totally B saturated, they suffice to demonstrate the pronounced variations in the total core-level line shape that are characteristic of this surface structure.

The top curve was collected near threshold (kinetic energy is equal to 6 eV), and under these conditions, the bulk-to-surface ratio attains its maximum value due to the relatively long electron-escape depth at low energy. With a photon energy of 120 eV, the kinetic energy of the photoelectrons is approximately 16 eV, close to the threshold for plasmon excitation, and consequently the bulk-to-surface ratio becomes smaller. The bottom two spectra are taken near the minimum in the escape-depth curve and in both cases the bulk-to-surface ratio is less than one. Between 130 and 140 eV (kinetic energies of 26 and 36 eV, respectively) the bulk-to-surface ratio does not change significantly; however, it does increase again above electron kinetic energies of 36 eV.

The bulk-to-surface peak areas have been plotted in the lower portion of Fig. 3. This plot resembles the “universal escape-depth curve” with the characteristic flat minimum around kinetic energies of 30–40 eV. Howev-

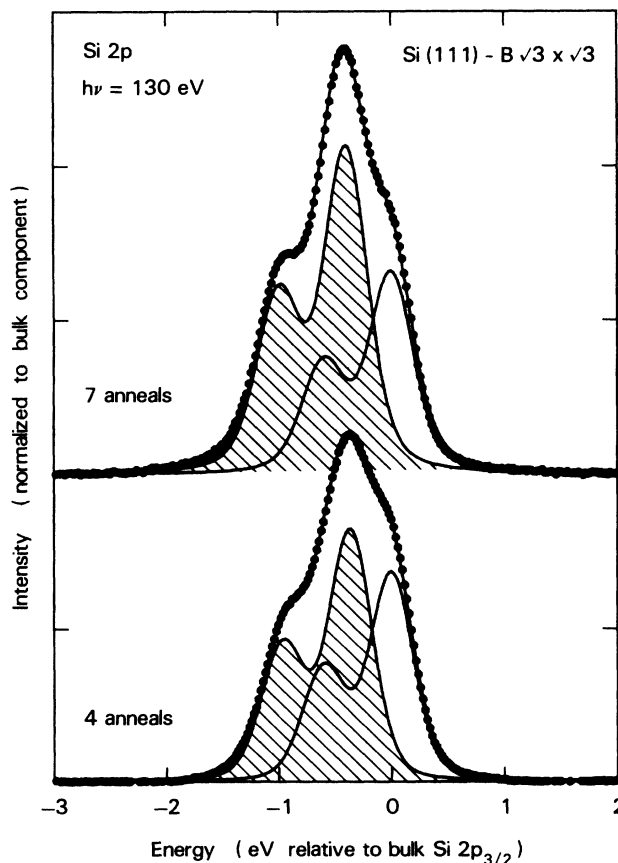


FIG. 1. Si 2*p* core-level spectra for Si(111)-B( $\sqrt{3}\times\sqrt{3}$ )R30° comprise a bulk component and, at lower energy, a Si-B surface component (hatched). The surface-to-bulk intensity ratio is higher than for any other Si surface studied to date. This points towards a subsurface site where the B can interact with two Si layers instead of one, as for a surface site. Repeatedly annealing highly B-doped Si(111) at  $\approx 1050^\circ\text{C}$  for 10–20 s segregates B to the surface region until saturation sets in at the ( $\sqrt{3}\times\sqrt{3}$ )R30° structure.

er, the intensity ratio is not the quantity of primary interest. It would be more useful to express the intensity ratio as a photoelectron escape depth or to use existing estimates of the escape depth to make some predictions about the surface geometry. To facilitate this, some assumptions about the spatial distribution of the surface atoms have to be made and we will turn to this next.

First, it will be demonstrated that the intensity ratios that we have extracted from least-squares analysis of the Si  $2p$  core level are inconsistent with  $\frac{1}{3}$  ML of B in adatom sites. To simplify the analysis it will be assumed that the Si bilayers are coplanar and separated by an average bulk distance of  $\approx 3.1$  Å. Cross-section variations are ig-

nored. Using a discrete-layer model, and assuming that the B adlayer saturates every dangling bond in the uppermost Si layer, leads to the following simple expression for the Si-B to bulk Si intensity ratio ( $R_{[111]} = I_{\text{Si-B}}/I_{\text{bulk}}$ ),

$$R_{[111]} = (1 - q_{[111]}) / (1 + q_{[111]}),$$

where the layer attenuation factor  $q_{[111]} = \exp(-d/\Lambda)$ ,  $d$  is the average (111) interplanar spacing, and  $\Lambda$  is the photoelectron escape depth. In the notation of Ref. 14,  $d = d_{[111]} + d'_{[111]}$ . Under surface-sensitive conditions, the escape depth in Si(111) lies within the range 3.0–4.0 Å.<sup>14,15</sup> Therefore, the surface-to-bulk intensity ratio will be calculated for  $\Lambda = 3$  Å and  $\Lambda = 4$  Å. This will define a range within which the surface-to-bulk intensity ratio should lie if the model provides a good description of

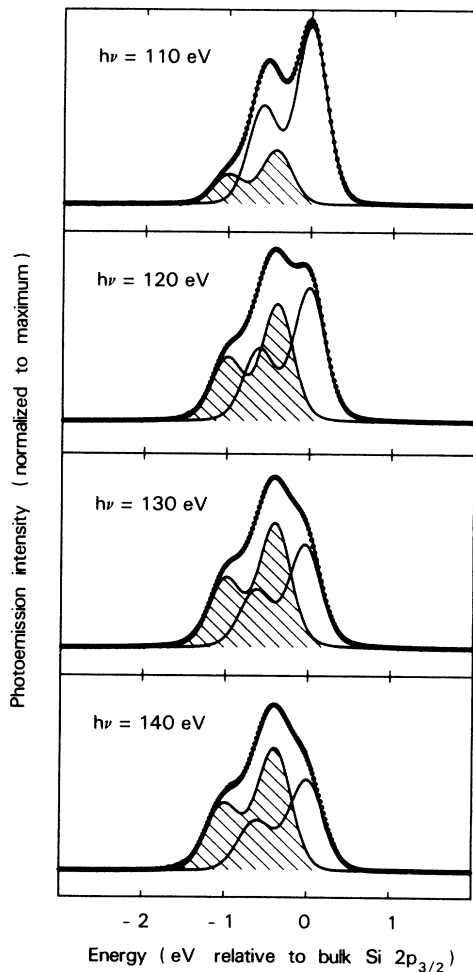


FIG. 2. The ratio of the Si-B to the bulk Si component can be altered by changing the kinetic energy of the outgoing photoelectrons. Under bulk-sensitive conditions (top curve) the bulk Si component is five–six times larger (by area) than the Si-B component. Under surface-sensitive conditions (bottom two curves) the situation reverses, and the magnitude of the Si-B component (hatched) is larger than that of the bulk Si component. This indicates that there are a large number of Si–B bonds in the surface region. The third spectrum ( $h\nu = 130$  eV) is the same as the bottom curve of Fig. 1.

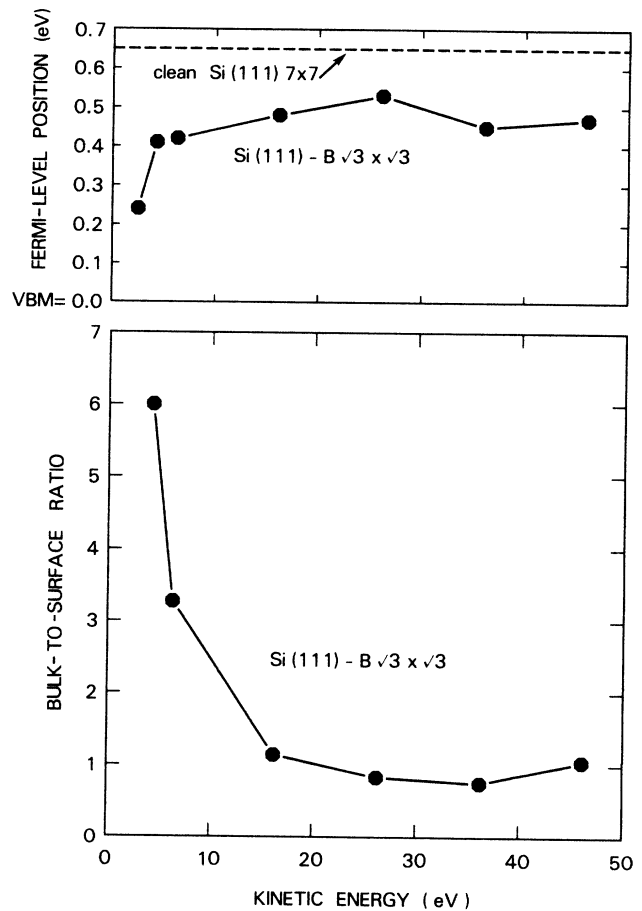


FIG. 3. The ratio of the bulk-to-surface (Si-B) intensity of the Si  $2p$  level vs the kinetic energy of the emerging photoelectrons (bottom curve) resembles the “universal escape-depth curve.” The apparent Fermi-level position (top curve) at the Si(111)-B( $\sqrt{3} \times \sqrt{3}$ ) $R 30^\circ$  structure approaches the bulk value (the valence-band maximum) under bulk-sensitive conditions due to the short depletion-layer width (57 Å). Under surface-sensitive conditions it approaches the surface value of 0.5 eV above the valence-band maximum (VBM).

the atomic positions at the surface. Substituting  $\Lambda=3$  Å and  $\Lambda=4$  Å in the above expression produces intensity ratios of 0.48 and 0.37, respectively. The range  $R_{[111]}=0.37-0.48$  lies substantially below the value that we have determined from least-squares analysis of the Si 2*p* core-level line shape ( $1.60\pm 0.04$ ). This pronounced discrepancy suggests that the adatom surface geometry does not provide a satisfactory description of this surface structure. Basically, the surface-to-bulk intensity ratio cannot be accounted for by simply assuming that B bonds only to 1 ML of Si atoms.

The second structure that will be considered has been found to give a good description of out-of-plane surface-x-ray-diffraction results<sup>6</sup> and has also been favored by LEED studies.<sup>10</sup> Moreover, first-principles pseudopotential calculations<sup>8,9</sup> have also identified it as the most thermodynamically stable surface geometry. The structure has B in a substitutional site, in the first Si bilayer, directly below a Si adatom in the  $T_4$  site. It has been proposed<sup>8,9</sup> that, due to the relatively short Si—B bond length, this configuration relieves subsurface strain. The surface should also be electrically passive due to charge transfer from the Si adatom to the substitutional B.<sup>8,9</sup>

To calculate the intensity ratio that we would expect from this structure, some simplifying assumptions will again be made. First, since only one surface component is observed in the Si 2*p* core level, it will be assumed that all of the Si atoms bonded to B atoms, and the Si adatoms in the  $T_4$  site, have the same binding energy. Although the Si adatoms are not nearest neighbors of the B atoms, they are within bonding distance because the B 1*s* core level has enough overlap with the Si adatom site to give a strong B 1*s* absorption (see later). Second, it will be assumed that the Si adatoms are coplanar with the first Si bilayer. Third, as before, it will be assumed that the Si bilayers are coplanar and separated by 3.1 Å. In addition, it has to be determined whether the extent of the B influence extends to all the Si atoms in the first bilayer or only to those Si atoms that the B is directly bonded to. We will consider the latter case first. Using a discrete-layer model, and assuming that only 1 ML of Si atoms in the first Si bilayer contribute to the shifted component results in the following expression:

$$R_{[111]} = (4 + q_{[111]}) / [2 - q_{[111]} + 6q_{[111]}(1 - q_{[111]})^{-1}] .$$

Substituting  $\Lambda=3$  Å and  $\Lambda=4$  Å into the above expression produces intensity ratios of 0.74 and 0.67, respectively. Although the intensity ratios ( $R_{[111]}=0.67-0.74$ ) have increased by almost a factor of 2 relative to the B-adatom model, the range lies well below the experimental value of  $1.60\pm 0.04$ . Consequently, if it is assumed that the shifted component in the Si 2*p* core level arises from the  $\frac{1}{3}$  ML of Si adatoms, 1 ML of Si atoms in the first bilayer (i.e., those the B bonds to directly), and  $\frac{1}{3}$  ML of Si atoms below the B layer, then the intensity ratio is still significantly smaller than the experimental value.

Assuming now that all the Si atoms in the first Si bilayer (including the second ML which does not bond to

the B directly) contribute to the intensity of the shifted component results in the following expression:

$$R_{[111]} = (6 + q_{[111]}) / [-q_{[111]} + 6q_{[111]}(1 - q_{[111]})^{-1}] ,$$

and the value for the intensity ratio is now 2.20 for  $\Lambda=3$  Å and 1.39 for  $\Lambda=4$  Å, defining the range  $R_{[111]}=1.39-2.20$ , which is in much better agreement with the experimental value of  $1.60\pm 0.04$ . Solving the above equation numerically suggests that the experimental value of 1.60 is reproduced by an escape depth of 3.65 Å, in good agreement with other estimates of the escape depth in this energy range.<sup>14,15</sup> Therefore, it is most likely that the shifted Si 2*p* component arises from  $\frac{1}{3}$  ML of Si adatoms,  $\frac{5}{3}$  ML of Si atoms in the first Si bilayer, and  $\frac{1}{3}$  ML of Si atoms below the B layer, then good agreement with the experimental value is obtained. This finding implies that the range of influence of the incorporated B layer extends to more than 1 ML of Si atoms.<sup>16</sup>

We now turn to consider the binding energy of the Si 2*p* core level. Unlike the Si(111)-(7×7) reconstruction, it was found that the binding energy of the Si 2*p* core level on the Si(111)-B( $\sqrt{3}\times\sqrt{3}$ )R30° reconstruction exhibited a weak dependence on the incident photon energy. To quantify this, the binding energy of the Si 2*p* core level was measured relative to the binding energy of the Si 2*p* core level on the Si(111)-(7×7) surface under identical conditions. Since the Fermi-level position within the Si band gap has already been determined for the 7×7 reconstruction (0.65 eV,<sup>13</sup> see also Ref. 17), we can use the difference between the two Si 2*p* binding energies to determine the Fermi-level position for the Si(111)-B( $\sqrt{3}\times\sqrt{3}$ )R30° surface reconstruction. The results are presented in the upper portion of Fig. 3.

It is clear from Fig. 3 that our estimate of the Fermi-level position is correlated with the variation of the photoelectron escape depth (using  $1/R_{[111]}$  as a measure of the escape depth). When the photoelectron escape depth is shortest (30–40 eV), the apparent position of the Fermi level within the Si band gap is highest. This is to be expected, because the *p*-type Si(111) wafers that we used were degenerately doped, and consequently the depletion region is relatively small. For example, in the depletion approximation the width of the depletion region at zero bias is  $\approx (2\epsilon_s V_b / qN_A)^{1/2}$ , where  $\epsilon_s$  is the dielectric constant of Si,  $V_b$  is the distance between the Fermi level and the valence-band maximum at the surface,  $q$  is the electronic charge, and  $N_A$  is the bulk doping density. Substituting  $V_b=0.5$  eV (see Fig. 3) gives a depletion width of  $\approx 57$  Å. This is extremely short, and a significant portion of the depletion region will be probed under bulk-sensitive conditions. For example, in the depletion approximation, at a distance of 10 Å from the surface,  $E_F - E_{VBM}$  will reduce to  $\approx 0.34$  eV. At 20 Å from the surface, the Fermi level will lie  $\approx 0.22$  eV above the valence-band maximum. This is qualitatively what is observed in the upper portion of Fig. 3. Consequently, due to the fact that the Si bands bend appreciably over the probing depth, it is not possible to determine the Fermi-level position within the Si band gap for the Si(111)-

$B(\sqrt{3} \times \sqrt{3})R30^\circ$  reconstruction with a high degree of precision. The value that we have obtained under surface-sensitive conditions ( $E_F - E_{\text{VBM}} = 0.5$  eV) is almost certainly an underestimate. It is quite possible that the Fermi-level position is actually pinned by bare patches of  $7 \times 7$ , since the perfect Si(111)- $B(\sqrt{3} \times \sqrt{3})R30^\circ$  structure should not exhibit any pinning states in the gap.<sup>8</sup> For comparison, the pinning position of the Si(111)- $(7 \times 7)$  reconstruction is shown in Fig. 3 as a dotted line 0.65 eV above the valence-band maximum.<sup>13,17</sup>

#### IV. 1s CORE-LEVEL PHOTOEMISSION AND ABSORPTION EDGE

Photoemission from the B 1s core level was observed from the Si(111) surfaces after several annealing cycles to 1050°C. The magnitude of the B 1s core level could be used as a measure of the amount of B present in the surface region. As with the Si-B component in the Si 2p core level, the B 1s intensity also saturated after five-ten annealing cycles. The binding energy of the B 1s core-level, relative to the Fermi level, was estimated to be 187.5 eV, with a relatively large uncertainty of  $\pm 0.5$  eV which arises predominantly from uncertainty in the monochromator calibration.

We also found that the B 1s edge contained a relatively sharp feature in *p* polarization. In Fig. 4 we have plotted the B 1s absorption edge, measured using the B 1s Auger-electron yield, in both *p* and *s* polarization. For reference (dotted line in Fig. 4) we also collected a spectrum from lightly doped *n*-type Si under identical conditions. Figure 4 shows clearly that the sharp feature at  $h\nu = 188.6 \pm 0.5$  eV and the relatively broad feature at  $\approx h\nu = 191$  eV are not present in pure Si. It also demonstrates the pronounced polarization dependence of the feature at  $h\nu = 188.6$  eV. The intensity of this feature is much stronger in *p* polarization, when the electric field vector of the incident light (see inset) is parallel to the surface normal. Dipole selection rules suggest that this feature has  $s-p_z$ -like symmetry. The angular dependence of this feature was studied in more detail and the normalized intensity, above background, is plotted against the polar angle (defined in the inset) in Fig. 5. Also plotted in Fig. 5, for reference, is a curve of form  $\sin^2(\theta)$ . The position of this feature suggests that it is an unoccupied level lying  $1.6 \pm 0.5$  eV above the valence-band maximum.

Both the energy position of this feature and its polarization dependence suggest that it is the empty dangling-bond orbital of the Si adatom in the  $T_4$  adatom site. The fact that this feature is seen in the B 1s edge suggests that there is some wave-function overlap between the Si adatom and the B under the  $T_4$  site. In fact, this observation agrees well with first-principles band calculations,<sup>8,9</sup> which show charge density on the Si adatom and on the B atom underneath for this surface state. It also has  $p_z$ -type character in the calculations, in agreement with our polarization-dependent results.

The other broad feature in the B 1s absorption edge at  $h\nu \approx 191$  eV also demonstrates a dependence on polar angle. However, it is in the opposite sense. Due to the

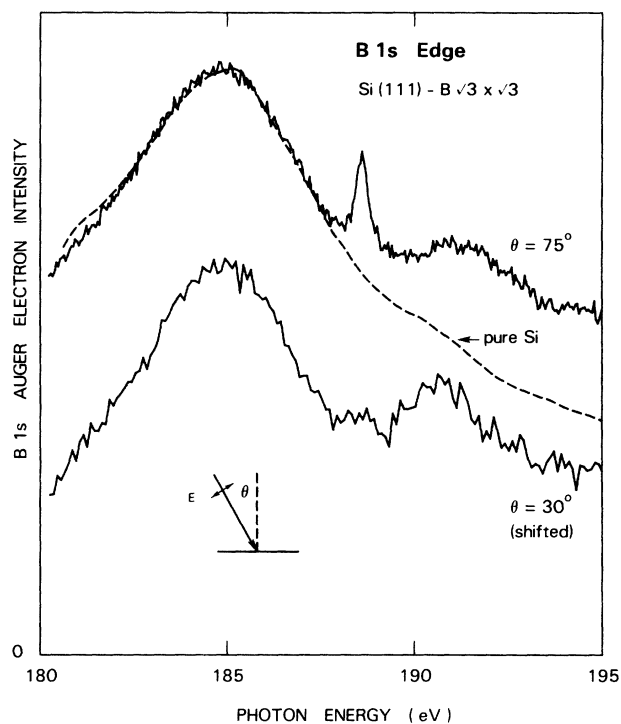


FIG. 4. The B 1s absorption edge measured using the B 1s Auger yield (kinetic energy = 175 eV and band pass = 8 eV). The absorption edge contains a polarization-dependent feature at  $h\nu = 188.6 \pm 0.5$  eV which has its maximum intensity when the electric field vector of the incident light is close to the Si(111) surface normal. It is assigned to a transition from the B 1s level into an empty surface state that is shared between the B atom and the Si adatom above it.

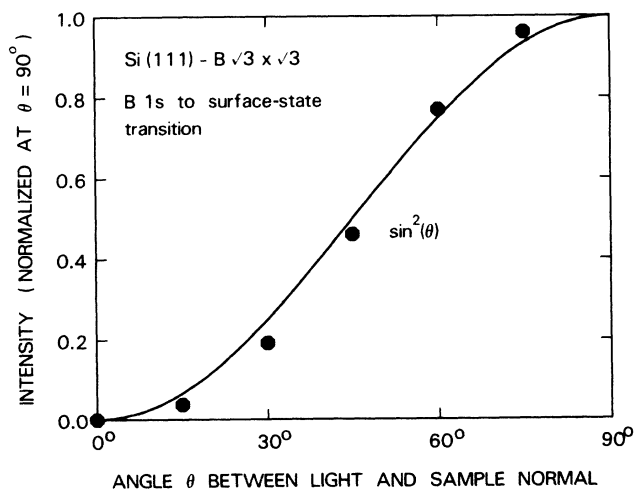


FIG. 5. The intensity of the sharp feature at  $h\nu = 188.6$  eV, above the background, has been plotted vs the polar angle. The feature attains its maximum intensity in *p* polarization and the angular dependence closely follows a function of form  $\sin^2\theta$ , corresponding to  $A_1(s, p_z)$  symmetry.

difficulties involved in reliably subtracting a background for this broad feature, its normalized intensity has not been included in Fig. 5.

### V. BURIED B LAYER AND $\delta$ DOPING

In order to study the transition from a near-surface B layer to a bulk dopant we covered the surface with a few layers of Si by dosing a sample with 10 000 L of Si<sub>2</sub>H<sub>6</sub> and annealing above the H desorption temperature. There were two motivating factors which dictated this approach. Firstly, CVD allows epitaxial growth at very low temperature<sup>18</sup> and, consequently, this prevents the B layer from diffusing. Secondly, pure Si has a tendency to island on the B-saturated surface. This is because the surface energy of clean Si is much higher than that of the B-saturated surface, which does not have partially filled broken bond orbitals.

Figure 6 shows that the B 1s absorption feature that we have attributed to the unoccupied adatom orbital persists upon growing a few layers of Si on top of it. However, it loses its polarization dependence and becomes completely

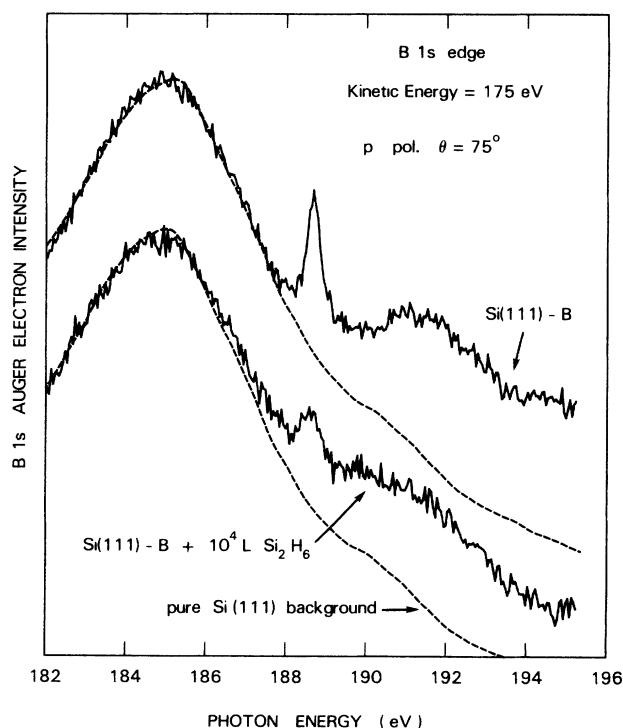


FIG. 6. The B 1s edge from the Si(111)-B( $\sqrt{3} \times \sqrt{3}$ )R30° surface is compared to that of the same surface covered by a few layers of Si using a chemical-vapor deposition (CVD) process. The sharp transition to an empty state persists, but loses its polarization dependence (not shown), since B is now in an isotropic bulk site.

isotropic (not shown). This is what we would expect from a B atom in a tetrahedral bulk doping site. It is interesting to compare the bonding configuration of the unoccupied orbitals in both cases. With a  $\frac{1}{3}$  ML of B atoms in subsurface sites, the B atom nominally picks up an electron from the filled-adatom Si dangling-bond orbital. When the B layer is buried several atomic layers beneath the surface, the B atom acts as an acceptor and takes on an electron from the surrounding Si lattice. In both cases, the empty B 2p state interacts with a Si neighbor to produce an empty orbital that is seen in soft x-ray absorption.

In the future, it would be interesting to study the orbitals of more dilute species, such as dopants or impurities, using core-level spectroscopy. From Figs. 4 and 6 one can see the limitation of the current technique, which uses the detection of Auger electrons to become sensitive to a small number of foreign atoms. The background from the direct Si valence-band photoemission (dashed lines) already is larger than the signal from  $\frac{1}{3}$  ML of B atoms. Going to lower concentrations of boron will require new techniques, such as background-free fluorescence detection. This is difficult due to the low fluorescence yield of shallow core levels.

### VI. CONCLUSIONS

We have studied the Si(111)-B( $\sqrt{3} \times \sqrt{3}$ )R30° reconstruction of the Si(111) surface using both Si 2p and B 1s core-level photoemission. A least-squares analysis of the Si 2p core-level line shape indicates that the Si 2p core-level comprises only one surface component. The intensity of the surface component, relative to the bulk component, is used to test surface structural models and to determine the Si-B bonding. The experimental intensity ratio is consistent with a substitutional model, where  $\frac{1}{3}$  ML of B atoms occupy Si sites below the T<sub>4</sub> site, and a simple adatom model, where  $\frac{1}{3}$  ML of B atoms reside in adatom sites. However, it is necessary to assume that Si atoms in the first double layer, including the Si atoms not directly bonding to B, are chemically shifted. This suggests either that the range of influence of the B atoms extends further than nearest neighbors, or that there is more than  $\frac{1}{3}$  ML of B in the surface region. It is possible, for example, that the second Si bilayer contains some B atoms that we have not accounted for in our analysis. This possibility cannot be ruled out *a priori* because most of the experimental studies that have been performed to date have focused only on the modification of the first Si bilayer, and they have not investigated the possible modification of deeper Si layers in any detail.

We have identified a sharp, polarization-dependent feature in the B 1s absorption edge above the Fermi level with *s-p<sub>z</sub>* symmetry that is attributed to an electronic transition from the B 1s level to the unoccupied dangling-bond orbital of the Si adatom. After covering the B layer with Si the angular anisotropy of this transition vanishes, as would be expected from a bulk dopant in an isotropic site.

## ACKNOWLEDGMENTS

The technical assistance of J. Yurkas and A. Marx is gratefully acknowledged. The research was carried out,

in part, at the National Synchrotron Light Source, Brookhaven National Laboratory (Upton, NY), which is supported by the U.S. Department of Energy (Division of Materials Sciences and Division of Chemical Sciences of the Office of Basic Energy Sciences).

- <sup>1</sup>J. M. Nicholls, B. Reihl, and J. E. Northrup, *Phys. Rev. B* **35**, 4137 (1987).
- <sup>2</sup>H. Hirayama, T. Tatsumi, and N. Aizaki, *Surf. Sci.* **193**, L47 (1988).
- <sup>3</sup>V. V. Korobotsov, V. G. Lifshits, and A. V. Zotov, *Surf. Sci.* **195**, 466 (1988).
- <sup>4</sup>F. Thibaudau, Ph. Dumas, Ph. Mathiez, A. Humbert, D. Satti, and F. Salvan, *Surf. Sci.* **211/212**, 148 (1989).
- <sup>5</sup>S. Bensalah, J. P. Lacharme, and C. A. Sébenne, *Surf. Sci.* **211/212**, 586 (1989).
- <sup>6</sup>R. L. Headrick, L. C. Feldman, and I. K. Robinson (unpublished); R. L. Headrick, I. K. Robinson, E. Vlieg, and L. C. Feldman, *Phys. Rev. Lett.* **63**, 1253 (1989).
- <sup>7</sup>P. Bedrossian, R. D. Meade, K. Mortensen, D. M. Chen, J. A. Golovchenko, and D. Vanderbilt, *Phys. Rev. Lett.* **63**, 1257 (1989).
- <sup>8</sup>E. Kaxiras, K. C. Pandey, F. J. Himpsel, and R. Tromp, *Phys. Rev. B* **41**, 1262 (1990).
- <sup>9</sup>I. W. Lyo, E. Kaxiras, and Ph. Avouris, *Phys. Rev. Lett.* **63**, 1261 (1989).
- <sup>10</sup>H. Huang, S. Y. Tong, J. Quinn, and F. Jona, *Phys. Rev. B* **41**, 3276 (1990).
- <sup>11</sup>D. E. Eastman, J. J. Donelon, N. C. Hien, and F. J. Himpsel, *Nucl. Instrum. Methods* **172**, 327 (1980).
- <sup>12</sup>F. J. Himpsel, Y. Jugnet, D. E. Eastman, J. J. Donelon, D. Grimm, G. Landgren, A. Marx, J. F. Morar, C. Oden, R. A. Pollak, and J. Schneir, *Nucl. Instrum. Methods* **222**, 107 (1984).
- <sup>13</sup>F. J. Himpsel, B. S. Meyerson, F. R. McFeely, J. F. Morar, A. Taleb Ibrahimi, and J. A. Yarmoff, in *Core-Level Spectroscopy at Silicon Surfaces and Interfaces*, Proceedings of the International School of Physics "Enrico Fermi," Course on Photoemission and Absorption Spectroscopy of Solids and Interfaces with Synchrotron Radiation, Varenna, 1988 (North-Holland, Amsterdam, in press).
- <sup>14</sup>F. J. Himpsel, F. R. McFeely, A. Taleb Ibrahimi, and J. A. Yarmoff, *Phys. Rev. B* **38**, 6084 (1988).
- <sup>15</sup>J. F. Morar, U. O. Karlsson, J. A. Yarmoff, D. Rieger, F. R. McFeely, and F. J. Himpsel (unpublished). The escape depths were obtained from an analysis of the Si 2*p* core-level photoemission from monolayer coverages of Cl on Si(111). The same electron analyzer and sample configuration were used in the present study.
- <sup>16</sup>This situation is not entirely satisfactory, because we would return to the adatom model and assume that the range of influence extends to all the atoms in the first bilayer, and not only to the Si atoms to which the B atoms are directly bonded. This would lead to an intensity ratio of  $R_{[111]} = (1 - q_{[111]})/q_{[111]}$ , and substituting  $\Lambda = 3 \text{ \AA}$  and  $\Lambda = 4 \text{ \AA}$  produces  $R_{[111]} = 1.86$  and  $1.17$ , respectively. The range  $1.17 - 1.86$  also contains the experimental value of  $1.60 \pm 0.04$ . Furthermore, the experimental intensity ratio is reproduced by a reasonable escape depth of  $3.20 \text{ \AA}$  (compare Refs. 14 and 15). We can say, however, that the observed Si 2*p* surface-to-bulk intensity ratio suggests that the range of influence to the B atoms appears to extend to Si atoms to which the B atoms are not directly bonded. This conclusion applies to both the adatom model, where there is  $\frac{1}{3}$  ML of B atoms in adatom sites, and to the substitutional model, in which the B atoms occupy the substitutional site below the  $T_4$  adatom site.
- <sup>17</sup>F. J. Himpsel, G. Hollinger, and R. A. Pollak, *Phys. Rev. B* **28**, 7014 (1983).
- <sup>18</sup>B. S. Meyerson, F. K. LeGoues, T. N. Nguyen, and D. L. Harnam, *Appl. Phys. Lett.* **50**, 113 (1987).